Evaluation and Design for an Integrated Modular Motor Drive (IMMD) with GaN devices

Jiyao Wang
Dept. of Electrical and Computer Engineering
University of Wisconsin- Madison
Madison, WI, USA
jwang229@wisc.edu

Ye Li
Dept. of Electrical and Computer Engineering
University of Wisconsin- Madison
Madison, WI, USA
lye6@wisc.edu

Yehui Han
Dept. of Electrical and Computer Engineering
University of Wisconsin- Madison
Madison, WI, USA
yehui@engr.wisc.edu

***Abstract*—this paper explores the use of GaN MOSFETs and series-connected inverter segments to realize an IMMD. The proposed IMMD topology reduces the segment voltage and offers an opportunity to utilize wide bandgap 200V GaN MOSFETs. Consequently, a reduction in IMMD size is achieved by eliminating inverter heat sink and optimizing the choice of DC-link capacitors. Gate signals of the IMMD segments are shifted (interleaved) to cancel the capacitor voltage ripple and further reduce the capacitor size. Motor winding configuration and coupling effect are also investigated to match with the IMMD design. An actively controlled balancing resistor is programmed to balance the voltages of series connected IMMD segments. Furthermore, this paper presents simulation results as well as experiment results to validate the proposed design.**

I. INTRODUCTION

Integrated modular motor drive has been shown to have great advantages in applications that require high efficiency and high power density. Without extra transmission cables, the cost of IMMD is lower, fault-tolerant and radiated EMI performance is better. The modularized design is also attractive because of the lower cost in manufacturing and maintenance [1] [2].

Traditional approaches to design such a compact system may face many challenges. Heat sinks and passive components, especially the DC-link capacitors, occupy a large portion of converter volume. The height and size of the heat sinks and capacitors limit the performance of traditional IMMD. In this paper, we propose a new IMMD design that can reduce the height and size of capacitors and eliminate the heat sinks of IMMD. Illustrated by Fig 1, semiconductor devices share the same heat sinks with machine. Considering relatively high machine operating temperature (about 90°C to 110°C for oil cooling), semiconductor devices must have superior efficiency and higher maximum junction temperature than conventional silicon power devices. It has been proved theoretically and experimentally that wide bandgap GaN devices can meet this stringent requirement [4] [9]. Besides, bulky capacitors take up to 30% of the total converter volume [5], and they are the highest components in IMMD. As in [1] and [2], traditional IMMD cannot fully integrate all the DC-link capacitors because their large size and height may cause physical vibration. In [3] and [5], researchers have built IMMDs with smaller size capacitors by introducing gate signal interleaving technique to reduce the capacitor ripple current. Lower DC-link voltage is proposed because the choice of low voltage capacitor is more flexible and capacitor optimization is easier to achieve. As a result, capacitor height is lowered. However in many applications, the low voltage DC-link is unavailable because it is supplied by a frontend passive rectifier, of which the voltage is fixed and decided by the power grid. Even in an application that the DC-link voltage (supplied by an active rectifier or a buck converter) could be lower, the overall system performance is degraded because a system with a constant power rating, lower voltage and higher current usually has a higher conduction loss and lower efficiency.

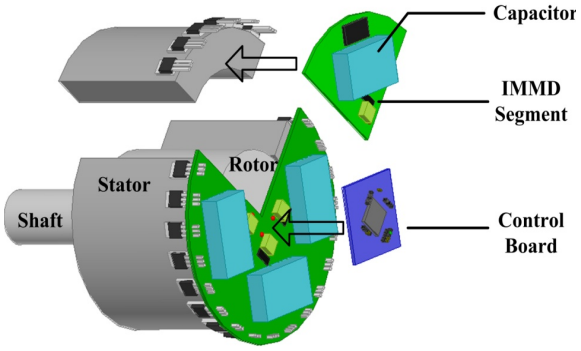

Fig. 1. Illustration of IMMD

The target of this research is to keep the height of capacitors within 1 inch and utilize GaN MOSFETs to eliminate the heat sinks. For these two reasons, each IMMD segment is rated below 200V. Several IMMD segments are connected in series to maintain the total DC-link voltage to be relatively high (400V for two segments and 600V for three segments). Moreover, IMMD segments can be interleaved to further reduce capacitor size. In this paper, comparison between the conventional motor drive and our proposed design is presented in section II. Section III covers the investigation of capacitor volume under different rating voltages. The size of electrolytic/film capacitor in the traditional motor

drive and our proposed IMMD are compared. In section IV, we introduce an active balancer that can balance the voltage of series connected IMMD segments. Finally, simulation and experiment results are shown to validate the proposed design.

II. PROPOSED IMMD STRUCTURE

A. Winding configuration

A properly designed IMMD should depend on the motor configuration. Their electrical and physical properties are matching with each other tightly. A motor usually has several pole-pairs and several slots in each phase. Windings in these pole-pairs and slots can be split into several branches in accord with certain rules. Different branches may locate in different poles, or in the same pole but different slots. For the sake of simplification, we consider only two branches of winding. The followings are two fundamental winding configurations suitable for IMMD.

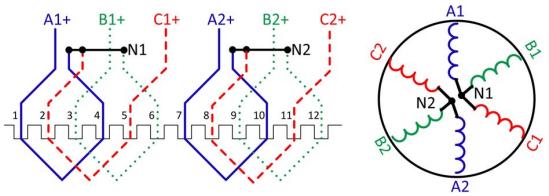

(a)

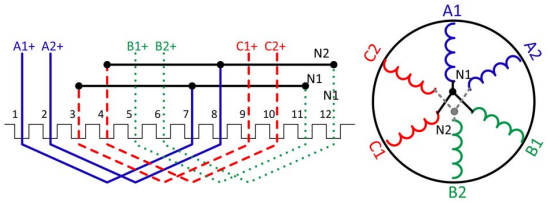

(b)

Fig. 2. Winding branches configuration. (a) In different poles (b) In the same pole but different slots

To clearly identify the two fundamental winding configurations, most simplified examples are presented in Fig. 2. Fig. 2(a) illustrates a 3 phases, 4-pole and 12 slots motor (1 slot per pole per phase). The windings in different pole pair are split into two branches. The two winding branches are usually connected in series or parallel in a normal machine so these branches share the same output terminals. However for IMMD design, the windings in different pole pairs are separated and have their own neutral points N1 and N2, output terminals A1 and A2. This configuration does not change any motor electrical property or induce extra cost but provides us with more flexibility to install an IMMD.

The second fundamental configuration is shown in figure 2(b), the distributed lap winding coils in a 3-phase, 2-pole and 12-slot motor (2 slots per pole per phase) is split into two branches. They should be series connected in a conventional motor to form a lap winding configuration. In IMMD design, the winding coils in two adjacent slots are completely separated and can be controlled individually.

In a real IMMD design, these two configurations can be combined and form into a more complicated one. For example, a machine with 4-pole, 2 slots per pole per phase could be split into 4 winding branches. 2 branches are split as Fig. 2(a) and the other two are split as Fig. 2(b). These configurations also open the opportunity for controlling motor in a more refined way [2].

B. IMMD segment connection

As illustrated in Fig. 3 (a), conventional motor drive has one inverter to drive all the winding branches. In Fig 3(b), conventional IMMD segments are connected in parallel. Although the machine winding can be altered to accommodate a wide range of voltage level, with GaN MOSFETs, all the IMMD segment rating voltages has to be under 200V. These winding branches lead to a compromise that the DC-link voltage has to be low and the DC-link current is high. The triangle carrier of PWM gate signal in each IMMD segments are shifted such that the total IMMD ripple current is reduced [5]. Thus a smaller capacitor can be substituted for the original one. Fig 3(c) illustrates our proposed IMMD. The segment rating voltage is identical to Fig 3(b) but the total system rating voltage is equivalent to Fig 3(a). Following advantages will make our proposed IMMD a powerful tool for driving motors.

(1) The gate signals of two IMMD segments are interleaved, and bring about a reduction in capacitor size for a specified dc bus voltage ripple.

(2) Unlike conventional motor drives, maintenance cost of IMMD is less expensive because the broken components only affect one segment. Fault condition is easier to detect.

(3) The design is flexible to accommodate the machine. An IMMD design can be the combination of Fig. 3(b) and Fig. 3(c). Even when the input DC-link voltage/current is given, there is extra room for varying the IMMD segment rating voltage/current. This is especially important in some applications when the DC-link voltage is high and suitable GaN device is unavailable.

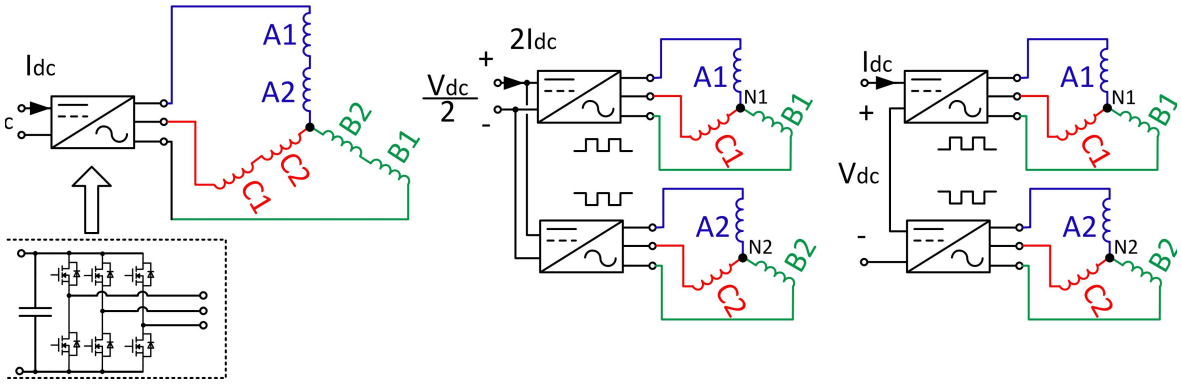

Fig. 3. (a) Conventional motor drive (b) conventional IMMD (c) the proposed IMMD

(4) The thermal performance is better. Several IMMD segments share the power and hence smaller devices with larger surface area per volume are used. The total surface area of semiconductor devices is increased.

(5) Lower IMMD segment voltage leads to a lower dv / dt in the machine slot insulation layer and hence tends to extend the machine lifespan.

(6) The size of IMMD is smaller and the height is reduced. GaN devices ($\approx$200V) can be used so that IMMD heat sink is eliminated. When the dc voltage is lower, the total volume of capacitance may not be reduced, but there are more choices of types of capacitors and more flexibility of the capacitor selection and optimization. As a result, the capacitors become more "flat" and the maximum height is reduced.

(7) The proposed IMMD can be matched with a multi-level frontend rectifier [13], which inherently has several capacitors connected in series.

C. Machine winding coupling effect

The winding branches are actually magnetically coupling with each other. The two fundamental configurations introduced in Fig. 2 have different magnetic property. Fig. 4(a) shows the corresponding magnetic equivalent circuit of the machine in Fig. 2(a). Two winding branches A1, A2 are in different poles and have negative coupling factor, i.e. M<0. If the rotor center shaft is not magnetizing, the coupling factor will be almost zero, but still negative.

Fig. 4(b) shows the case in Fig. 2(b). Since the winding branches are in the same phase and same pole, α (electrical angle between two windings) is less than 90°. Assume air-gap length, rotor diameter and motor length is g, D and L respectively. The coupling inductance could be calculated by:

$$M_{12} = \left(1 - \frac{2\alpha}{\pi}\right) DL \frac{\mu_0 N_{A1} N_{A2}}{2g} > 0$$

With gate signal interleaving technique, the magnetic coupling between branches will influence the output line current ripple. According to [6], M<0 results in smaller current ripple and M>0 has larger current ripple than M=0. These two cases can both be driven by IMMD segments but only the M<0 case is suitable for interleaving. If the winding branches in Fig 4(b) are driven by interleaving IMMD segments, there will be a large current ripple, leading to extra conduction loss.

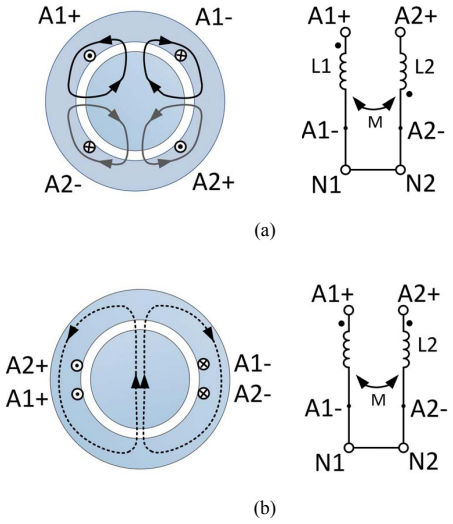

Fig. 4. (a) Winding branches in different poles (b) winding branches in the same pole but different slots

III. Capacitor Volume Evaluation

A. Capacitor volume v.s. switching frequency

Since the capacitors play a dominant role in reduction of IMMD volume, it is necessary to compare the capacitor size between conventional motor drives and IMMD. The switching frequency of motor drive ranges from 10 kHz to 40 kHz.

Before evaluating the capacitor volume, an important observation should be emphasized first: Electrolytic capacitor size is limited by the capacitor rating current (RMS value), not by the capacitance. This is because electrolytic capacitors usually have very large capacitance but small current rating. In other word, if an electrolytic capacitor is selected such that the current rating meets the requirement, its capacitance is far more than necessary. Take a three phase inverter as an instance, the capacitor current RMS value can be calculated by the following equation. From [7], the DC-link capacitor current can be approximately estimated as:

$$I_{Cap\_RMS} = I_{Line\_RMS}\sqrt{2M\left[\frac{\sqrt{3}}{4\pi} + \cos^2\phi\left(\frac{\sqrt{3}}{\pi} - \frac{9}{16}M\right)\right]} \approx 0.55 I_{Line\_RMS}$$

, where M is the modulation index and assumes to be 0.9 , cosΦ is the power factor and assumes to be unity.

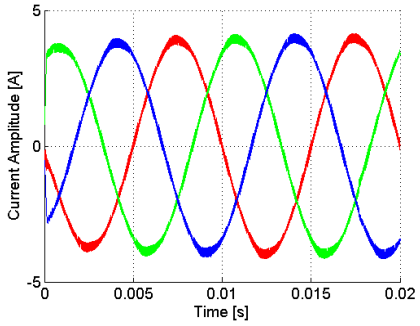

(a)

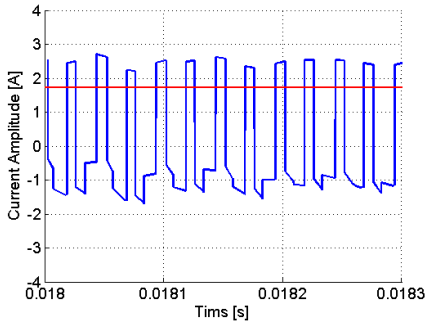

(b)

Fig. 5. IMMD with 20 kHz switching frequency. (a) Output line current waveform. (b) DC-link capacitor current with 1.80A RMS value.

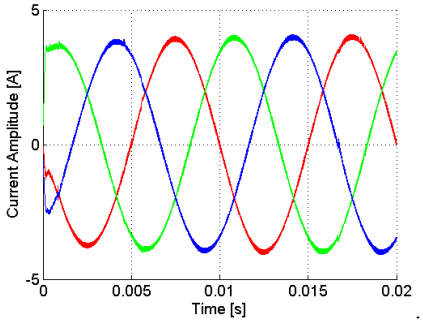

(a)

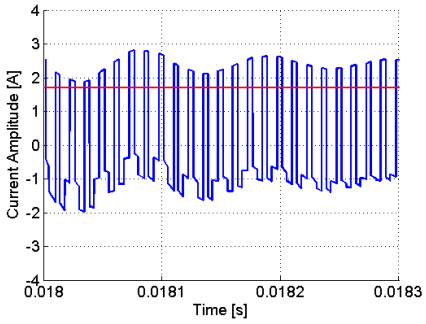

(b)

Fig. 6. IMMD with 40 kHz switching frequency. (a) Output line current waveform. (b) DC-link capacitor current with 1.78A RMS value.

TABLE I. Capacitor selection for 200V IMMD segment

Switching freq.	10kHz	20kHz	40kHz
Capacitor RMS current in Fig. 5(b) & Fig. 6(b)	1.86A	1.80A	1.78A
Max. voltage ripple limit	2V	2V	2V
Minimum capacitance needed	80uF	39μF	19μF
Electrolytic cap. type	250V Panasonic EETXB2E821KJ		
Capacitance	820μF		
RMS current rating	2.0A		
Volume	35325 mm^3		
Voltage ripple on capacitor	0.019	0.09V	0.046V
Film capacitor type	250V EPCOS 8 * B32524	250V EPCOS 4 * B32524	250V EPCOS 2 * B32524
Capacitance	80uF	40μF	20μF
RMS current rating	21.6A	10.8A	5.4A
Volume	67724 mm^3	33862 mm^3	16931 mm^3
Voltage ripple on capacitor	2V	2V	2V

The DC-link capacitor RMS current does not depend on switching frequency. Two simulation models can further illustrate this equation. These two models have identical voltage, current and power input/output. The only difference is the switching frequency-- Fig. 5 and Fig. 6 shows the 20 kHz and 40 kHz model respectively.

From the simulation results, although the frequency of DC-link capacitor current is in accord with the switching frequency, the RMS current value of DC-link capacitor does not change. If an electrolytic capacitor is selected for the 20kHz model, when the switching frequency is increasing to 40kHz, since the RMS current remains the same, the electrolytic capacitor cannot be reduced. But the voltage ripple in DC-link capacitor is reduced by half in the 40kHz model. TABLE I summarizes the electrolytic capacitor selection for the 10kHz, 20kHz and 40kHz model.

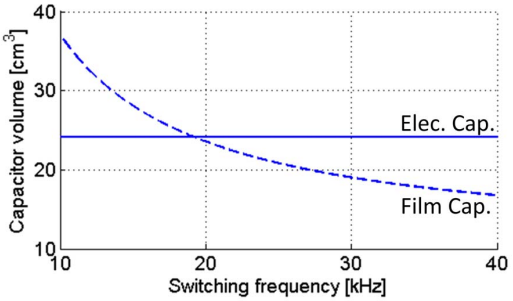

Fig. 7. The total volume of electrolytic capacitors and film capacitors in the 200V, 2.0A IMMD segment under different switching frequency.

From [8], the system usually has a 1% maximum voltage ripple requirement. The electrolytic capacitor selection is based on the RMS current rating. But the capacitance is much larger than needed, illustrated by TABLE I. In contrast, film capacitor and ceramic capacitor have much smaller capacitance per volume than electrolytic capacitor, but larger RMS current rating. The selection of these capacitors is usually according to the maximum voltage ripple requirement. When the switching frequency is increasing, smaller capacitance is sufficient and the capacitor size can be reduced. TABLE I also shows the selection for film capacitor. From the comparison, film capacitors have better performance than electrolytic capacitors in terms of the size.

For low power and low vibration application, ceramic capacitors are also promising candidates because of their compact size. The performance of ceramic capacitors is similar to the film capacitor. However, due to the material characteristics, large size ceramic capacitors are easy to crack, unlike the film and electrolytic capacitors that have self-heal ability. Therefore it is undesirable to use ceramic capacitors for DC-link in a high power IMMD.

B. Gate signal interleaving technique

The duty of DC-link capacitors is to stabilize the DC-link voltage and to smooth the input current [5]. In the conventional IMMD shown in Fig. 3(b), two IMMD segments have interleaving gate signals, meaning that the gate signals of two IMMD segments have identical duty ratio, but are shifted by 180° from each other. Then the DC-link current ripple can be reduced. Compared with non-interleaving IMMD segments, the interleaving IMMD segments will have an equivalent higher switching frequency, and thus can have smaller DC-link capacitors while maintain the same voltage ripple on Vdc.

The interleaving technique can also be applied to the proposed IMMD shown in Fig. 3(c). The gate signals of two IMMD segments are shifted by 180°, like in the conventional IMMD. Instead of reducing the total current ripple on DC-link, the proposed IMMD will reduce the total DC-link voltage ripple. The voltage ripples on both IMMD segments are combined because they are connected in series. The voltage ripple amplitude will be reduced and the equivalent frequency is twice the switching frequency. In other word, smaller DC-link capacitors can be used to maintain the same voltage ripple on the input terminals.

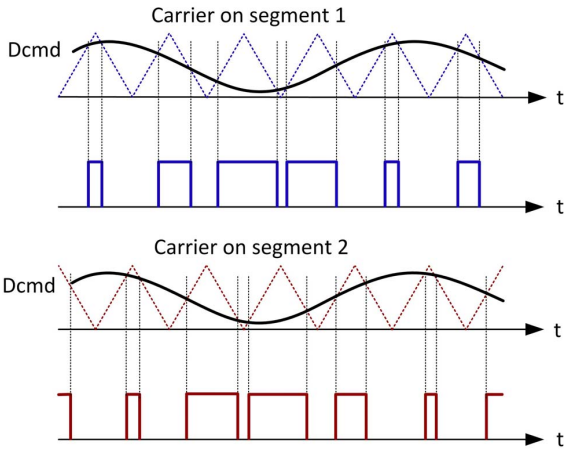

Fig. 8. Illustration of gate signal interleaving. The duty ratio commands of both IMMD segments are identical.

IV. ACTIVE VOLTAGE BALANCER

The IMMD segments are connected in series and supplying independent machine windings. Due to machine asymmetry or unbalanced load condition, each independent machine winding may have different electric properties and cause the voltages of IMMD segments unequal. The unbalanced machine winding degrades the fault tolerance and control stability of the IMMD. In extreme case, it may cause inverter damage when the IMMD segment voltage exceeds the maximum allowable voltage. To prevent this from happening, control algorithm has been applied to IMMD to balance the segment voltages. Similar work has been done in Input-Series-Output-Parallel DC-DC converters [11] [12]. To control the series-connected segment voltage, controller will adjust the duty ratio command such that each segment has identical power outputs. For IMMD, the idea of controlling the segment voltage is similar. But it is different from DC-DC converters since both d-axis and q-axis are involved in the AC system.

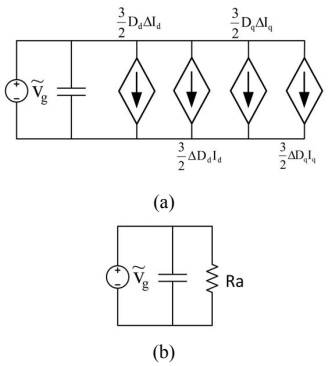

Fig. 9. (a) Input small signal model of one IMMD segment. (b) The equivalent small signal model of active voltage balance resistor.

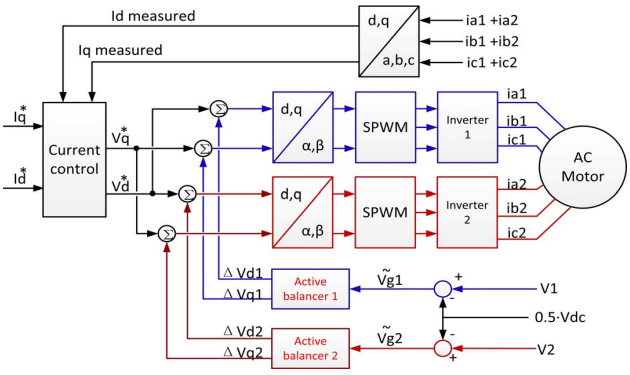

Fig. 10. Active balancer block diagram

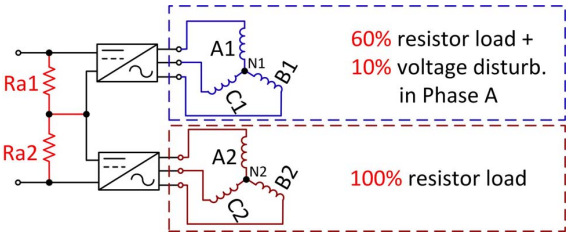

Fig. 11. Active balancer equivalent circuit

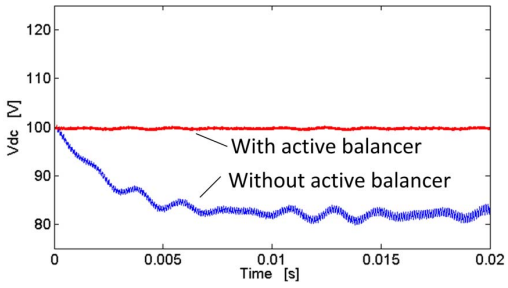

(a)

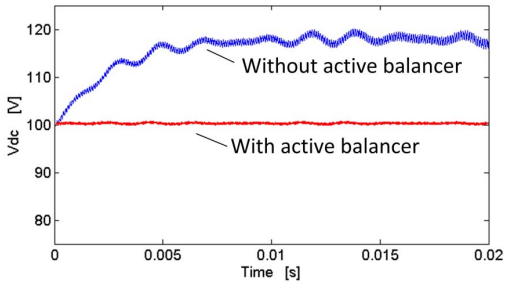

(b)

Fig. 12. Two segments IMMD with 200V total DC-link voltage (a) The DC-link voltage on segment 1. (b) The DC-link voltage on segment 2.

Capacitors connected in series are usually balanced by passive resistors connected in parallel with the capacitors. These passive resistors are usually large and in the range of 10kΩ to 200kΩ. The current balancing capability of these resistors is smaller than 1 mA. This is enough for balancing the capacitors since the capacitor leakage current is smaller than 1μA. In an IMMD, the current difference can be as large as 1A so the passive resistors have to be smaller than 10Ω to balance the voltage. It is unachievable to install these resistors otherwise the steady state Ohmic loss of the system will be tremendous. Inspired by the work in [10], an actively controlled resistor is realized in the control algorithm to balance the IMMD segment voltage. Fig. 9(a) shows the input small signal model for a three-phase inverter [14], where $\tilde{v}_g$ is the unbalanced voltage error. To realize an active balance resistor, the duty ratio is manipulated intentionally. Fig. 9(a) and Fig. 9(b) will be equivalent when the controller is applied. Under this situation, the following equation must be satisfied. The current small signal can be neglected because the current loop has much slower dynamic response than the voltage balance resistor.

$$\frac{\tilde{v}_g}{R_a} = \frac{3}{2}\Delta D_d I_d + \frac{3}{2}\Delta D_q I_q \qquad \text{(Eq. 1)}$$

The controller is built as Fig. 10, and it will perform as balance resistors as shown in Fig. 11. The resistors Ra1 and Ra2 are programmed to 1Ω. The value of ΔDd and ΔDq in Eq. 1 can be various choices. In this paper, we prefer to the minimum square root values, i.e.

$$\Delta D_d = \frac{\tilde{v}_g}{\frac{3}{2}R_a\sqrt{\left(I_d^{\,2}+I_q^{\,2}\right)}}\cdot I_d$$

$$\Delta D_q = \frac{\tilde{v}_g}{\frac{3}{2}R_a\sqrt{\left(I_d^{\,2}+I_q^{\,2}\right)}}\cdot I_q$$

and $\Delta D_q^{\,2}+\Delta D_d^{\,2}$ is minimum.

As indicated by Fig. 11, the machine windings may have disturbance and unbalanced load, which causes unbalance segment voltage. The simulation results of IMMD voltage balancing is illustrated in Fig. 12. Without the active balancer, the upper segment 1 is supplying the same voltage as the lower segment 2, but the load current of segment 1 is larger than that of segment 2. Hence the

DC-link voltage of segment 1 will drop until the load current is identical as segment 2. With the active balancer, IMMD is able to reject the load disturbance and maintain equal DC-link voltage on each of the IMMD segments.

V. Simulation and Experiment Results

A. Simulation of SPM machine closed loop control

In simulation, the controller is built as Fig. 10, and the balance resistors Ra1 and Ra2 are programmed to 1Ω. Fig. 13 shows the simulation results of SPM machine constant torque start up. These simulation results have proved that the segment driver works properly for the standard closed loop torque control and the voltage is balanced equally.

TABLE II. Simulation machine parameters

Vdc	200 [V]
Machine inductance (Ld and Lq)	1.015 [mH]
Voltage constant	49.2 [Vpp/krpm]
Torque constant	0.407 [N.m/A_peak]
Pole	4

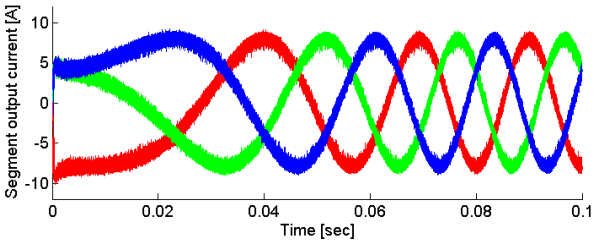

(a)

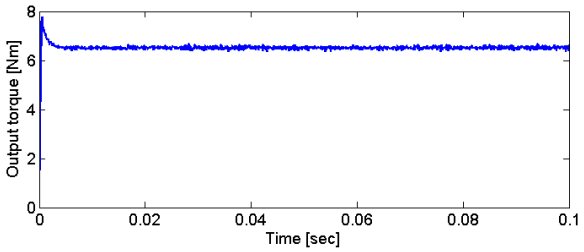

(b)

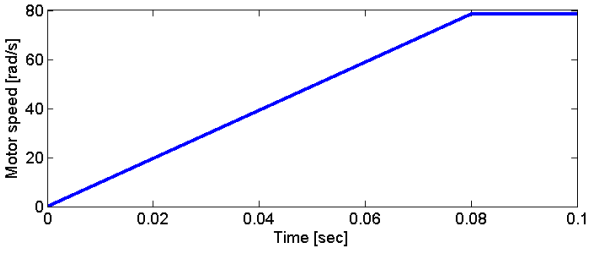

(c)

Fig. 13. Simulation results of IMMD. (a) Three phase output current waveforms. (b) Output shaft torque of the machine. (c) Motor speed.

B. Experiment results of the prototype IMMD

TABLE III. Prototype IMMD specifications

Vdc	180 [V]
Line current	7 [Arms]
DC-Link capacitance	36 [μF]
Converter height	0.6 [inch]
IMMD radius	3 [inch]

Two IMMD segments are built and each of them is rated at 180V, 7A. The segment driver is equipped with isolated digital voltage and three phase current measurements. Instead of driving a motor, prototype GaN IMMD drives an RL load for test propose. 50Hz three phase currents are produced by IMMD segment, as shown in Fig. 14(b). Due to device availability, experiments shown in Fig. 14(c) and (d) are using traditional MOSFETs with larger current rating. The voltage on each IMMD segment is automatically balanced, as illustrated in Fig. 14(c). The benefit of interleaving is also validated, because experiment results in Fig. 14(d) shows at least 35% reduction in the DC-link current ripple.

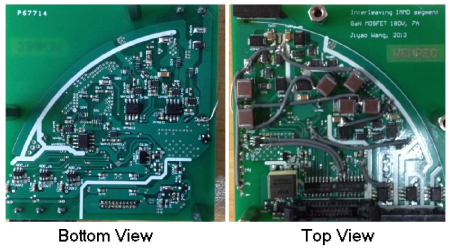

(a)

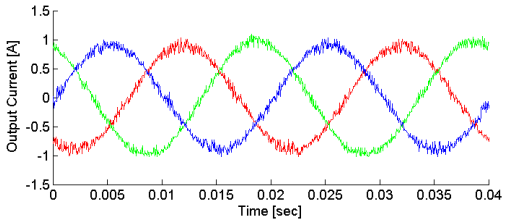

(b)

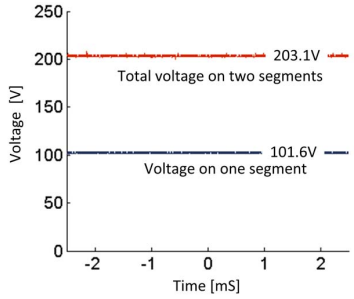

(c)

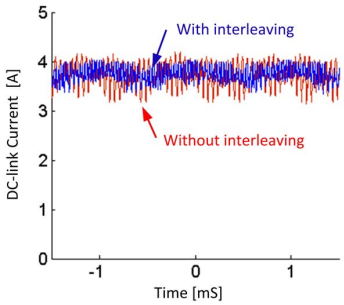

(d)

Fig 14. Experiment results. (a) Photograph of GaN IMMD prototype. (b)Three phase output current waveforms. (c) Voltage balance between two segments. (d) DC-link current comparison between IMMD with and without interleaving.

VI. Conclusion and Future Work

This paper investigates interleaving IMMD segment design and evaluates the total capacitor volume. Very compact IMMD design could be reached via 1) appropriate interleaving gate signals by 180° to reduce the voltage ripple and capacitor size, 2) utilization of GaN devices to eliminate IMMD heat-sinks, and 3) increase the switching frequency to reduce the capacitor volume. The proposed IMMD proves to be feasible through simulation and experiment results.

Future work may include 1) further integration of control unit on the segment and 2) the design of front-end rectifier.

REFERENCES

[1] N.R. Brown, T.M. Jahns and R.D. Lorenz, "Power Converter Design for an Integrated Modular Motor Drive", *IAS'07*, pp.1322-1328, Sept 2007.

[2] B.J. Skyora, T.M. Jahns and R.D. Lorenz, "Development of a Demonstrator Model of an Integrated Modular Motor Drive", *NSF-CPES'08*, April 2008.

[3] S.C. Tang, D.M. Otten, T.A. Keim, and D.J. Perreault, "Design and Evaluation of a 42-V Automotive Alternator With Integrated Switched-Mode Rectifier", *VPPC'07*, pp.250-258, Sept. 2007

[4] T. Morita, S. Tamura, Y. Anda, M. Ishida, Y. Uemoto, T. Ueda, T. Tanaka and D. Ueda, "99.3% Efficiency of Three-Phase Inverter for Motor Drive Using GaN-based Gate Injection Transistors", APEC'11, pp.481-484, 2011

[5] G. Su and L. Tang, "A Segmented Traction Drive System with a Small dc Bus Capacitor", ECCE'12, pp.2847-2853, Sept. 2012

[6] Lit-Leong Wong, Peng Xu, P. Yang, and F.C. Lee, "Performance Improvements of Interleaving VRMs with Coupling Inductors Pit", *Power Electronics, IEEE Transactions,* pp. 499-507, July 2001

[7] J.W. Kolar, and S.D. Round, "Analytical Calculation of the RMS Current Stress on the DC Link Capacitor of Voltage DC Link PWM Converter Systems", *Electric Power Applications, IEE,* pp.535-543, July 2006

[8] M. Salcone, J. Bond, "Selecting Film Bus Link Capacitors For High Performance Inverter Applications:, IEMDC'09, pp.1692-1699, May 2009

[9] D. Ueda, M. Hikita, S. Nakazawa, K. Nakazawa, H. Ishida, M. Yanagihara, K. Inoue, T. Ueda, Y. Uemoto, T. Tanaka and T. Egawa, "Present and Future Prospects of GaN-Based Power Electronics", *ICSICT'08,* pp.1078-1081, Oct 2008

[10] H. Ertl, T. Wiesinger, and J.W. Kolar, "Active Voltage Balancing of DC-link Electrolytic Capacitors", *Power Electronics, IET,* pp.488-496, Dec. 2008

[11] J.W. Kimball, J.T. Mossoba and P.T. Krein, "A Stabilizing, High-Performance Controller for Input Series-Output Parallel Converters", *Power Electronics, IEEE Transactions,* pp.1416-1427, May 2008

[12] R. Ayyanar, R. Giri and N. Mohan, "Active Input-Voltage and Load-Current Sharing in Input-Series and Output-Parallel Connected Modular DC-DC Converters Using Dynamic Input-Voltage Reference Scheme", *Power Electronics, IEEE Transactions*, pp.1462-1473, Nov 2004

[13] C. Klumpner, F. Blaabjerg, and P. Thogersen, "Evaluation of the converter topologies suited for integrated motor drives", IAS'03, pp. 890-897, vol.2, Oct 2003

[14] S. Hiti, D. Boroyevich, and C. Cuadros, "Small-signal modeling and control of three-phase PWM converters", IAS'94, pp.1143-1150 vol.2, Oct 1994